ACS AGRICULTURAL SCIENCE & TECHNOLOGY

pubs.acs.org/acsagscitech

Article

Encapsulation of *Trichoderma harzianum* in Carboxymethyl Cellulose Reinforced with Nanocellulose for Delivery as Fertilizer Coatings

Aline M. Ferreira, Mariana G. Brondi, and Cristiane S. Farinas*

Cite This: *ACS Agric. Sci. Technol.* 2026, 6, 527−538

Read Online

ACCESS | Metrics & More | Article Recommendations | Supporting Information

ABSTRACT: The limited stability of microbial inoculants such as *Trichoderma harzianum* (*T. harzianum*) poses a major challenge to the development of effective delivery systems. To address this, a nanocomposite matrix of carboxymethyl cellulose (CMC) reinforced with cellulose nanocrystals (CNC) was developed to encapsulate *T. harzianum* and facilitate delivery through fertilizer granules. The encapsulation was highly effective; after three months of storage at room temperature, encapsulated spores maintained high viability (~6.5×10^8 CFU g^{-1}), whereas nonencapsulated spores exhibited a three-order-of-magnitude reduction. Incorporation of CNC also generated a sustained-release profile for the spores by enhancing the structural integrity of the CMC matrix and creating a more tortuous diffusion path. Moreover, the polymeric coating was essential for preserving fungal viability and promoting growth under the osmotic stress imposed by monoammonium phosphate (MAP) fertilizer even after 30 days of storage at room temperature. These findings highlight the potential of these formulations as protective and efficient delivery systems for microbial inoculants, improving their stability within integrated fertilization strategies.

KEYWORDS: *biocontrol, microbial viability, controlled release, encapsulated microorganism*

INTRODUCTION

Meeting the growing global demand for food, fiber, and bioenergy while ensuring environmental sustainability remains one of the major challenges of modern agriculture.[1] Chemical fertilizers and pesticides have played a key role in enhancing crop productivity and controlling pests and diseases. However, their intensive and prolonged use has led to severe environmental consequences, including reduced soil quality, nutrient losses through volatilization, leaching, and reactions with soil organic components, as well as compromised food quality.[2,3] These issues highlight the need for alternative methods based on natural, biodegradable, and sustainable resources.

Microbial inoculants have emerged as a promising solution by introducing beneficial microorganisms into agricultural systems to promote plant growth, inhibit phytopathogens,[4] and solubilize essential nutrients for plants.[5] Compared with conventional practices, microbial inoculation can enhance crop productivity while reducing the environmental burden associated with agrochemicals.[6] However, their widespread application is still limited by challenges related to low microbial viability over time and incompatibility with conventional fertilizers.[7]

The direct contact of microorganisms with high concentrations of fertilizers, such as monoammonium phosphate (MAP) or urea, poses significant risks to microbial survival and activity due to factors like osmotic stress, extreme pH variations, nutrient imbalances, and the presence of reactive chemical species. For instance, localized changes in salinity and alkalinity resulting from the dissolution of MAP or urea-based fertilizers have been shown to impair the viability of encapsulated microorganisms.[8] Therefore, developing formulation strategies to preserve microbial viability and enable coapplication with fertilizers is essential for the advancement of biological inputs.

Encapsulation in biodegradable polymeric matrices has shown great potential to overcome these challenges.[9−11] This approach provides a physical barrier that protects microbial cells and facilitates their combination with fertilizers. Among these polymers CMC stands out for its nontoxicity, biocompatibility, water solubility, renewable origin, and low cost, making it suitable for microbial encapsulation.[12] However, its limited mechanical strength has led researchers to explore reinforcement strategies.[13]

Cellulose nanocrystals (CNCs) have gained attention as effective reinforcing agents, significantly improving the mechanical properties of polymeric films. Reported strength increases of up to 400% and rigidity enhancements of about 20% have been achieved with CNC incorporation into CMC matrices.[14] CNCs have also demonstrated potential for microbial encapsulation, enhancing the shelf life and stress tolerance of *T. harzianum*, including resistance to heat, UV radiation, and fungicides.[9,15] Additionally, the structural integrity provided by CNCs makes these nanocomposites

Received: October 31, 2025
Revised: February 3, 2026
Accepted: February 6, 2026
Published: February 11, 2026

https://doi.org/10.1021/acsagscitech.5c00992
ACS Agric. Sci. Technol. 2026, 6, 527−538

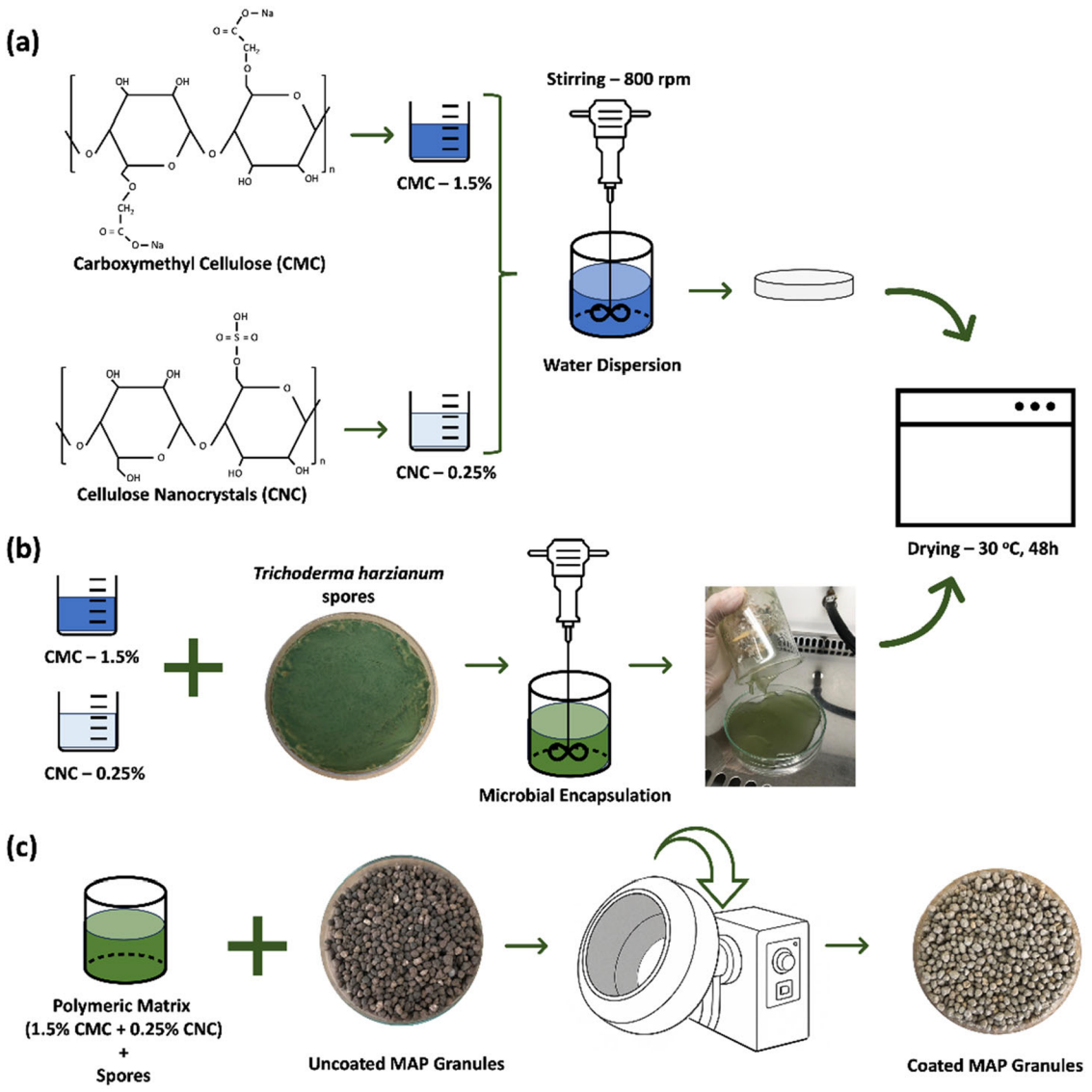

Figure 1. Schematic representation of the preparation of polymeric films by the casting method. (a) Without microorganism: dispersion of CMC and CNC in water stirred at 850 rpm for 5 h, followed by drying in an oven at 30 °C for 48 h; (b) with microorganism: the same procedure as in (a), including *T. harzianum* spores (10^9 spores g^{-1}); (c) schematic representation of the coating process for MAP fertilizer granules. The process involves mixing a polymer matrix containing CMC (1.5%), CNC (0.25%) and *T. harzianum* spores with uncoated MAP granules in a rotating pan coater under controlled temperature conditions.

suitable as protective coatings on fertilizers, allowing the codelivery of microbial inoculants and chemical inputs.

Therefore, this study aimed to develop and characterize polymeric matrices based on CMC reinforced with CNC for the encapsulation of the biocontrol agent *T. harzianum*. These matrices were applied as coatings on MAP fertilizer granules to create a multifunctional delivery system, enabling the coapplication of biological and chemical products while enhancing microbial viability and stability in agricultural applications.

MATERIALS AND METHODS

Materials

The encapsulating matrices were prepared using CMC (average viscosity, 2040 cps; degree of substitution, 0.7; molecular weight, 265,000 g mol^{-1}) obtained from Synth (Brazil). CNCs were used as a reinforcing agent and supplied by Celluforce (Canada). According to the manufacturer, the CNCs were produced by sulfuric acid hydrolysis (64% w/v), which introduced half-ester sulfate groups onto their surface. The CNCs exhibited a nominal average diameter of 7.5 nm, a length of 150 nm, and an aspect ratio (L/D) of approximately 20. *T. harzianum* LQC99, obtained from the Embrapa Meio Ambiente culture collection (Brazil), was selected as the model microorganism for encapsulation due to its well-established role as a biocontrol agent and plant growth promoter.[16,17] This species is widely recognized for its ability to enhance root development and nutrient solubilization while inducing systemic resistance in plants.[18,19]

Film Production

The polymeric films were produced using the casting method, which involved preparing the polymeric dispersion followed by oven drying. For CMC-only films, dispersions containing 1.5% CMC (w/v) in 100 mL of distilled water were stirred at 850 rpm for 5 h. Approximately 100 mL of the dispersion was then evenly distributed onto a Petri dish (diameter 21 cm) and dried at 30 °C in an oven without air circulation for 48 h, to prevent bubble formation (Figure 1a). For the reinforced films, CNC (0.25% w/v) was first dispersed in water under

https://doi.org/10.1021/acsagscitech.5c00992
ACS Agric. Sci. Technol. 2026, 6, 527−538

agitation (850 rpm) before the addition of CMC (1.5% w/v), following a similar protocol.

Microorganism Cultivation

The initial inoculum was prepared from stock cultures maintained at ultralow temperature (−80 °C). The cultures were resuspended and transferred to potato dextrose agar (PDA) plates, which were incubated in a BOD chamber at 28 ± 2 °C for 6 days. After incubation, spores were suspended in sterile saline solution (0.85% NaCl). The spore concentration was determined using a Neubauer counting chamber.[9]

Microorganism Encapsulation

To incorporate the microorganism into the matrices, all materials, except the polymers, were sterilized by autoclaving at 121 °C for 15 min. The process was conducted under sterile conditions in a laminar flow hood to avoid contamination. A spore concentration of 1.5×10^9 spores g^{-1} of polymer was added to both CMC (1.5%) and CMC:CNC nanocomposite (1.5% CMC and 0.25% CNC). The mixtures were stirred for 30 min to ensure homogeneity before being evenly spread onto Petri dishes. The films were dried in an oven at 30 °C for 48 h (Figure 1b).

Fungal Growth Assay on PDA

To evaluate the growth of the encapsulated microorganism, small films pieces (5 mm in diameter) were added to the center of a Petri dish containing PDA medium. The fungal growth was monitored for 6 days to assess whether encapsulation affected fungal development, comparing encapsulated spores with free spores. The films were placed under aseptic conditions in a laminar flow hood and incubated in a BOD chamber at 28 ± 2 °C for 6 days. The experiment was conducted in triplicate.

Spore Release from Films

The release of *T. harzianum* from the polymeric matrices was evaluated using film fragments. For this assay, 0.01 g samples of the encapsulated material were transferred to 125 mL Erlenmeyer flasks containing 10 mL of sterile saline solution (0.85% NaCl). The flasks were incubated in an orbital shaker at 30 °C and 250 rpm. Samples (10 μL aliquots) were collected at 0, 1, 2, 5, 15, and 30 days, and the spore concentration was quantified using a Neubauer chamber. The experiment was performed in biological duplicates and analytical triplicates.

Viability of Encapsulated Microorganism during Storage

The encapsulated materials were stored in zip lock bags under two temperature conditions: 4 °C (refrigerated) and room temperature, for a period of 3 months. Samples were collected at 0, 1, 2, and 3 months for analysis. To determine viability, 0.1 g of material was cut into small pieces and transferred to Erlenmeyer flasks containing 50 mL of saline solution (0.85% NaCl). Spore release was performed by incubating the flasks for 24 h at 30 °C. Subsequently, the samples were subjected to serial dilutions and inoculated onto PDA plates. Colony counts were performed after 24 h of incubation at 28 °C, and the Colony Forming Units per gram (CFU g^{-1}) were determined visually.

Coating of MAP Granules

MAP granules (diameter: 2.8−3.3 mm) were provided by Adubos Vera Cruz Ltd.a (Brazil). Three different coating formulations were prepared for application: a CMC matrix, a CMC:CNC matrix, and a sugar syrup control. The sugar syrup treatment was included as a proxy for traditional on-farm practices, in which simple adhesives or carbon-rich solutions are commonly used to attach microbial powders to seeds or solid fertilizers.[20,21] First, the polymeric dispersions were loaded with the microorganism. A spore concentration of 1.5×10^9 spores g^{-1} of polymer was incorporated into both the CMC (1.5% w/v) and the CMC:CNC nanocomposite (1.5% CMC and 0.25% CNC) dispersions. For the control, a solution was prepared by dissolving 10 g of sugar in 100 mL of water at 100 °C. After the solution cooled to 30 °C, 6.6 mL of a *T. harzianum* suspension was added to achieve a final concentration of 1.5×10^9 spores g^{-1}. This procedure ensured that the total spore load was consistent across all treatments, allowing direct comparison between the polymer based protective matrices and the conventional adhesive approach.[22] The coating process followed the methodology by Bortoletto-Santos et al.,[23] (Figure 1c). Briefly, 150 g of MAP granules were placed in a coating pan rotating at 30 rpm, with heated airflow maintained at 30−35 °C. A total of 10% by mass of the respective coating dispersion (polymer-to-fertilizer ratio) was applied to the granules using a Pasteur pipet. The morphology of the coating layer formed on the granules was analyzed using SEM.

Fungal Growth from Coating Process

The ability of the fungus to grow from the coated granules was evaluated under two experimental conditions: (i) immediately after coating and (ii) after a one month storage period. For the initial condition, MAP granules were tested 24 h after the coating process. For the storage condition, a separate batch of coated granules was stored for 30 days at room temperature in sealed bags prior to testing. In both cases, a single coated granule was placed in the center of a Petri dish containing oat culture medium. The plates were then incubated at 28 ± 2 °C in BOD, and fungal growth was monitored for 6 days. All assays were conducted in triplicate under sterile conditions.

Scanning Electron Microscopy (SEM) on Films without and with Microorganisms

The surface morphology of the films was evaluated by Scanning Electron Microscopy (SEM) (JEOL JSM-6510). Samples were mounted on aluminum stubs, secured with carbon adhesive tape, and coated with a thin layer of gold using an ion sputter coater (BALTEC Med. 020). The SEM analyses were performed at an acceleration voltage of 5 kV using a secondary electron detector.

Thermogravimetric Analysis (TGA) and Differential Scanning Calorimetry (DSC) on Films without and with Microorganisms

The thermal behavior of the films was evaluated by TGA and DSC (SDT−TA Instruments, Model SDT650). Approximately 5 mg of each sample was placed in a platinum crucible and heated from room temperature to 800 °C at a heating rate of 10 °C/min under a nitrogen atmosphere with a flow rate of 100 mL/min.

Fourier Transform Infrared Spectroscopy (FTIR) on Films without and with Microorganisms

The chemical characterization of the films was obtained by FTIR, using the Bruker Vertex 70 spectrometer equipped with an attenuated total reflectance (ATR) accessory. Spectra were recorded in the range of 4000−400 cm^{-1}, with 32 scans per sample at a resolution of 4 cm^{-1}. All spectra were normalized at approximately 1020 cm^{-1} for consistent comparison.

Mechanical Analysis

The tensile properties of the films (without microorganisms) were evaluated using a universal testing machine (EMIC, model DL-3000) equipped with a 50 kgf load cell. The analysis was performed based on ASTM standard D882−01, with five replicates for each sample. The initial grip distance was set at 12 cm, and the tensile speed was 25 mm/min. Maximum tensile strength, strain at break, and Young's modulus were determined from the resulting stress−strain curves using the equipment's software. Young's modulus was calculated from the slope of the initial linear region of the curve.

RESULTS AND DISCUSSION

Formulation Selection of the Films

To establish an optimal formulation for the encapsulation matrix, a preliminary screening was conducted by varying the concentrations of CMC and CNC, with the key observations summarized in Table 1. Representative images of the films obtained during this screening process, illustrating the transition from low structural integrity to optimal uniformity, are provided in Figure S1 (Supporting Information). First,

https://doi.org/10.1021/acsagscitech.5c00992
ACS Agric. Sci. Technol. 2026, 6, 527−538

Table 1. Preliminary Screening of Film Formulations and Their Observed Properties

CMC (%, w/v)	CNC (%, w/v)	observed characteristics
Screening of CMC Concentration		
0.5	0	low structural integrity and high friability
1.0	0	weakened structure; prone to fragmentation
1.5	**0**	good structural integrity and easy handling
2.0	0	high dispersion viscosity impairs processability
2.5	0	excessively high viscosity limits processability
Screening of CNC Concentration (with 1.5% CMC)		
1.5	0.1	properties similar to pure CMC; no significant changes
1.5	**0.25**	improved mechanical performance and visual uniformity
1.5	0.5	dispersion issues with visible aggregates
1.5	1.0	strong aggregation limits uniformity

different concentrations of pure CMC were evaluated. While lower concentrations (0.5% and 1.0% w/v) resulted in films with poor structural integrity, higher concentrations (≥2.0% w/v) produced dispersions with excessively high viscosity, which impaired processability. Consequently, 1.5% (w/v) CMC was selected as the optimal base concentration, as it provided good structural integrity and ease of processing and application. Subsequently, with the CMC concentration fixed at 1.5%, various concentrations of CNC were added as a reinforcing agent. The addition of 0.25% (w/v) CNC resulted in films with improved mechanical performance and visual uniformity. In contrast, higher CNC concentrations (≥0.5% w/v) led to visible aggregation and a nonuniform matrix. Therefore, the formulation composed of 1.5% CMC and 0.25% CNC was selected for all subsequent studies.

Morphological Characterization of the Films

The CMC and CMC:CNC matrices produced films with homogeneous morphology and sufficient structural integrity for handling and subsequent coating. As illustrated by the insets in Figure 2, there were distinct visual differences between the films with and without the microorganism. The films without *T. harzianum* were translucent and largely colorless (insets in Figure 2a,b). In contrast, films containing the encapsulated spores exhibited an opaque appearance and a distinct greenish aspect, attributable to the natural pigmentation of the fungus (insets in Figure 2c,d).

The surface morphology of the films without microorganisms is shown in Figure 2a,2b. Pure CMC films (Figure 2a) demonstrated a smooth, compact, and regular surface, with no detectable defects within the resolution limits of the SEM analysis. In contrast, CMC:CNC nanocomposite films (Figure 2b) exhibited some surface particulates, likely related to challenges in achieving complete CNC dispersion within the polymeric matrix. Although these particulates are not uncommon in nanocomposite formulations, their presence, particularly at higher concentrations, can act as localized stress points and affect mechanical performance.[24] Nevertheless, their limited presence in the selected formulation for this study did not appear to compromise the overall integrity of the films, as discussed in subsequent sections.

In the films containing microorganisms (Figure 2c–2f), *T. harzianum* spores were successfully encapsulated within the polymeric matrices. The incorporation of the microorganism resulted in alterations to the surface morphology, resulting in increased heterogeneity and the presence of visible particles corresponding to the fungal spores (Figure 2e,2f). The spores displayed a uniform size of approximately 2 μm calculated using ImageJ software (Figure 2e,2f), aligning with the dimensions reported by Muñoz-Celaya et al.,[25] These results indicate the efficacy of the encapsulation process.

Thermogravimetric Analysis (TGA)

The thermal stability of the films (without and with microorganisms) was investigated using TGA, with the degradation curves and their derivatives (DTG) shown in Figure 3a,3b, respectively. All formulations exhibited a characteristic multistage degradation profile.

The first mass loss stage, occurring between 40 and 160 °C, corresponds to the evaporation of adsorbed water due to the hydrophilic nature of the polymers.[26] The initial thermal degradation event was observed to occur above 220 °C, resulting in mass losses ranging from ∼12% to ∼15%. These losses can be attributed to the degradation of the polysaccharide side chains and the release of CO_2.[27] The temperature range and the extent of mass loss observed are consistent with the thermal decomposition behavior of polysaccharides, where the scission of glycosidic bonds and

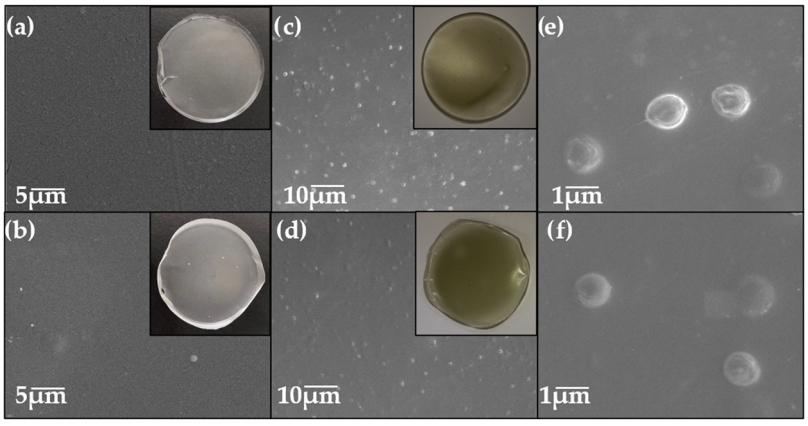

Figure 2. Scanning electron microscopy (SEM) micrographs of the surfaces of films. (a) without microorganism CMC film and (b) without microorganism CMC:CNC film. (c, e) CMC film with encapsulated *T. harzianum* at different magnifications. (d, f) CMC:CNC film with encapsulated *T. harzianum* at different magnifications. Insets show the corresponding visual appearance of each film.

https://doi.org/10.1021/acsagscitech.5c00992
ACS Agric. Sci. Technol. 2026, 6, 527−538

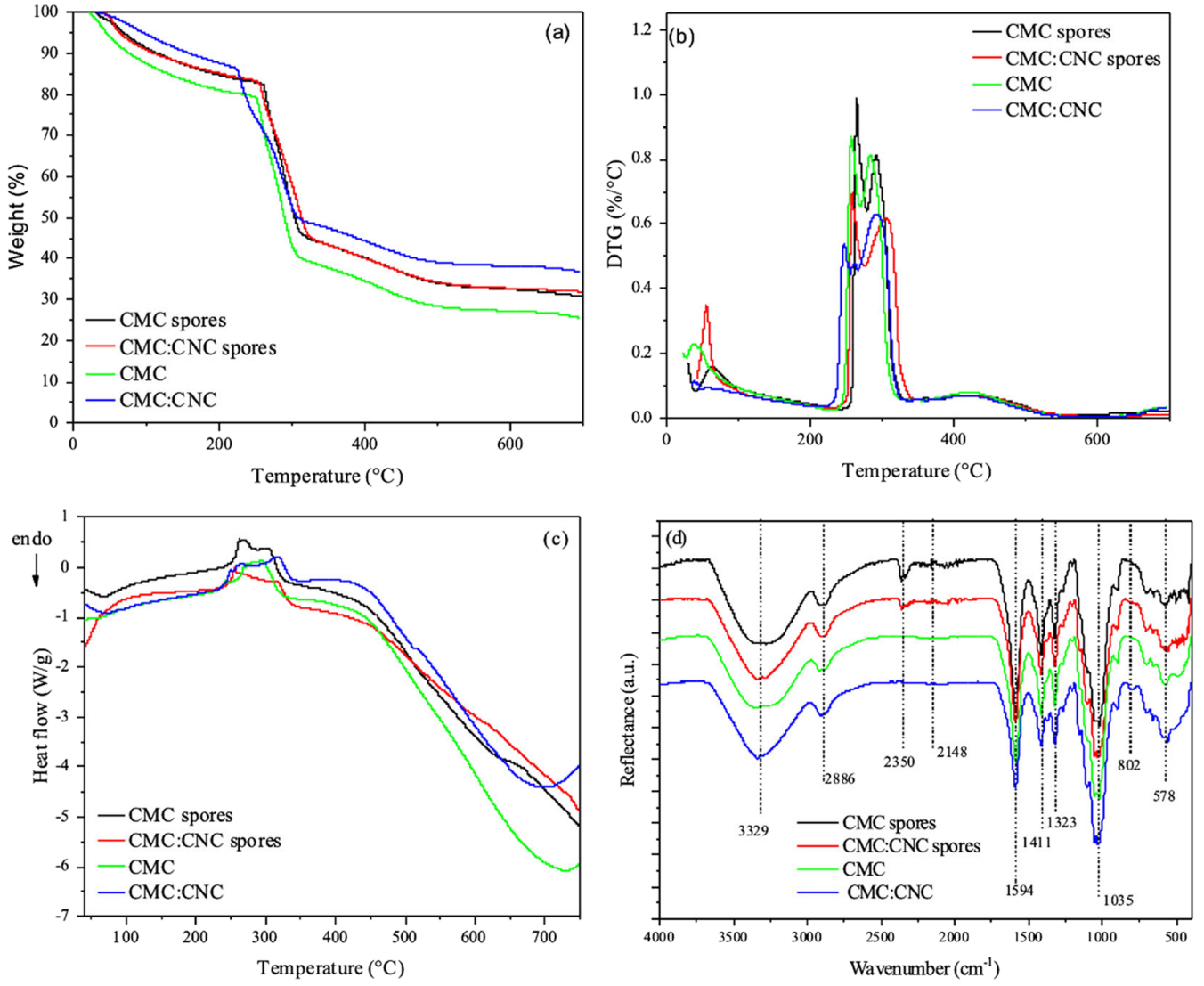

Figure 3. Thermal and chemical characterizations of CMC and CMC:CNC with and without microorganism: (a) Thermogravimetric analysis (TGA), (b) derivative thermogravimetry (DTG), (c) differential scanning calorimetry (DSC), and (d) Fourier transform infrared spectroscopy (FTIR) showing the thermal stability and chemical composition of the polymer matrices with and without the encapsulated microorganism.

the decarboxylation of functional groups are common processes.

In the second thermal degradation stage, which involved mass losses of ∼24% to ∼26%, the decomposition of the polymer's main chains was observed. This event aligns with findings from ref 28. Notably, the onset temperatures for the first and second thermal degradation events differed between the CMC:CNC nanocomposites and the pure CMC films. For the nanocomposites, the degradation began at ∼235 °C and ∼264 °C−274 °C (without and with microorganisms, respectively), whereas for the pure CMC films, it started at ∼245 °C and ∼268 °C−278 °C (without and with microorganisms, respectively). This difference is likely due to the presence of sulfate groups on the CNC surface, introduced during sulfuric acid hydrolysis. These groups can reduce the thermal stability of cellulose by facilitating dehydration reactions.[29]

Notably, the onset temperatures for thermal events were slightly lower for the CMC:CNC nanocomposites compared to pure CMC films. Despite this, CMC:CNC films demonstrated a 10% reduction in total mass loss, suggesting enhanced thermal stability due to interactions between CMC and CNC, aligning with findings from Kumar et al.,[30] and Yadav et al.[31] Furthermore, a 10% decrease in the total mass loss was observed in the CMC:CNC films, which highlights the formation of hydrogen bonds between CMC and CNC, as demonstrated by Mandal et al.[32]

The incorporation of *T. harzianum* into the polymeric matrices resulted in similar thermal behavior between the films without the microorganism. While minor differences in mass loss curves were observed, the overall profiles of the matrices remained comparable. As shown in Figure 3a, the substantial overlap in the thermal degradation curves suggests a strong interaction between the microorganism and the polymeric matrices.

Differential Scanning Calorimetry (DSC)

The thermal transitions of the films were further investigated by DSC, with the results presented in Figure 3c. Films (without microorganisms) showed two distinct endothermic events: a broad peak between 80−247 °C, corresponding to the evaporation of absorbed and bound water and a second

https://doi.org/10.1021/acsagscitech.5c00992
ACS Agric. Sci. Technol. 2026, 6, 527−538

peak between 247−340 °C, attributed to the thermal degradation of the polymer components.[33]

In contrast, films containing *T. harzianum* exhibited a prominent exothermic peak between approximately 150−340 °C, indicating overlapping degradation processes involving both the polymeric matrix and the microbial cells.[33] A comparison between CMC_{spores} and $CMC:CNC_{spores}$ formulations revealed that the peak degradation temperature for the nanocomposite (254 °C) was slightly lower than that of the CMC_{spores} film (260 °C). This finding is consistent with the TGA results and is likely attributed to the presence of sulfate groups on the CNC surface, which can catalyze cellulose degradation and thus lower the onset temperature.[33,34] Furthermore, the observed discrepancies in thermal profiles between films (with and without microorganisms) may also be due to the complex presence and/or interaction between the microorganisms and the polymeric matrices, potentially influencing the degradation pathways or altering the heat capacity of the system.

Fourier Transform Infrared Spectroscopy (FTIR)

The FTIR spectra of films formed from the dispersion of CMC materials and the nanocomposite, both with and without microorganisms, as shown in Figure 3d, exhibited characteristic cellulose bands and demonstrate a chemical structure similarity between CMC and CNCs, in accordance with the literature.[33,35]

For pure CMC films, the bands at 3329 cm^{-1} can be attributed to the stretching of hydroxyl groups (−OH) in cellulose.[9,33,35] The bands at 2886 cm^{-1} correspond to C−H stretching vibrations,[36] while the absorption band at 1594 cm^{-1} is due to the asymmetric stretching vibrations of the carboxylate group.[37] Bands at 1411 cm^{-1} and 1323 cm^{-1} are attributed to CH_2 stretching and −OH bending vibrations, respectively. The band ranging from 1035 cm^{-1} is associated with the C═O stretching in the polysaccharide backbone.[38]

The incorporation of CNCs into the polymeric matrices led to the appearance of a small, but characteristic, peak at approximately 810 cm^{-1} in the FTIR spectra of the nanocomposite films. This peak is typically attributed to the C−O−S group of sulfate ester present on the CNC surface,[9,39,40] providing direct evidence of the successful incorporation of CNCs into the CMC matrix. Despite this discernible feature, the overall spectral profile of the nanocomposites showed no other significant alterations, a result of the high degree of structural similarity between CMC and CNC, which causes their characteristic peaks to overlap, alongside the relatively low content of CNC within the nanocomposites.

Following the incorporation of the *T. harzianum* fungus into the matrices, two peaks at 2350 cm^{-1} and 2148 cm^{-1} appeared. These peaks are attributed to nitrogen bonds of the amide type, resulting from C−N stretching and N−H deformation vibrations in the amide group. This observation is consistent with the presence of proteins in the fungal structure, as microorganisms contain amino acids with characteristic amide bonds.[41]

This observation suggests a possible modification in the chemical composition or molecular interactions in the presence of *T. harzianum*, which may be relevant for characterizing and understanding the properties of the encapsulated polymeric films. A study by Maruyama et al.[42] also documented a single peak shift to 3681 cm^{-1}, suggesting an interaction between the fungus and microparticles during the encapsulation of *T. harzianum* in alginate beads.

Mechanical Analysis

Mechanical analysis is essential for evaluating the properties of polymeric films used in the encapsulation of microorganisms in agriculture, as it ensures the strength, flexibility, and integrity required to withstand handling, storage and field application. The incorporation of reinforcing agents, such as CNCs, has been reported to significantly enhance mechanical performance by preventing structural collapse and improving stress resistance.[26,43]

The mechanical behavior of CMC films and CMC:CNC nanocomposites was evaluated, and the results are summarized in Table 2. The incorporation of CNCs significantly improved both tensile strength and Young's modulus compared to the pure CMC film, indicating stronger and stiffer materials. The pure CMC film exhibited a tensile strength of 52.23 MPa and a Young's modulus of 1980.8 MPa, with an elongation at break of 6.58%, suggesting a material with moderate rigidity and flexibility. After CNC incorporation, the nanocomposite film reached a tensile strength of 94.39 MPa and a Young's modulus of 2886.0 MPa.

Table 2. Mechanical Properties of CMC and CMC:CNC Films[a]

films	tensile strength (MPa)	Young's modulus (MPa)	elongation at break (%)
CMC	52.23 ± 5.59[b]*	1980.8 ± 297.76[b]**	6.58 ± 1.66[a]
CMC:CNC	94.39 ± 8.13[a]*	2886.0 ± 506[a]**	2.95 ± 1.38[b]

[a]Different letters in the columns indicate a statistical difference according to the Tukey's test ($P < 0.05$). The letter accompanied by (*) and (**) refers to the statistics of the Young's Modulus and Elongation at break, respectively.

This considerable increase in strength and stiffness is primarily attributed to strong interfacial interactions between the functional groups of CMC (hydroxyl and carboxyl) and the hydroxyl groups on the CNC surface, resulting in the formation of hydrogen bonds.[32] Moreover, the introduction of new sulfate groups during sulfuric acid hydrolysis of CNCs can further enhance these interactions, contributing to the overall improvement in mechanical properties.[43,44]

Conversely, a reduction in elongation at break was observed in the CMC:CNC nanocomposite, from 6.58% in pure CMC to 2.95%. This behavior reflects the typical trade-off between flexibility and reinforcement, where the rigid nanocrystals restrict polymer chain mobility, thereby increasing tensile resistance while decreasing elongation capacity. Similar findings have been reported by El Achaby et al.,[35] who observed a significant enhancement in tensile strength and modulus after incorporating CNCs into CMC matrices, albeit at the cost of reduced flexibility.

It is also important to note that excessive CNC loading may lead to nanoparticle aggregation, impairing stress transfer and diminishing mechanical properties. Concentrations above 5% CNC have been associated with such detrimental effects.[35] Thus, the 0.25% CNC concentration used in this study appears to balance reinforcement and processability effectively.

Growth of the Microorganism in PDA and Release Profile

To confirm that the encapsulation process and subsequent storage did not impair fungal viability, a growth assay was

https://doi.org/10.1021/acsagscitech.5c00992
ACS Agric. Sci. Technol. 2026, 6, 527−538

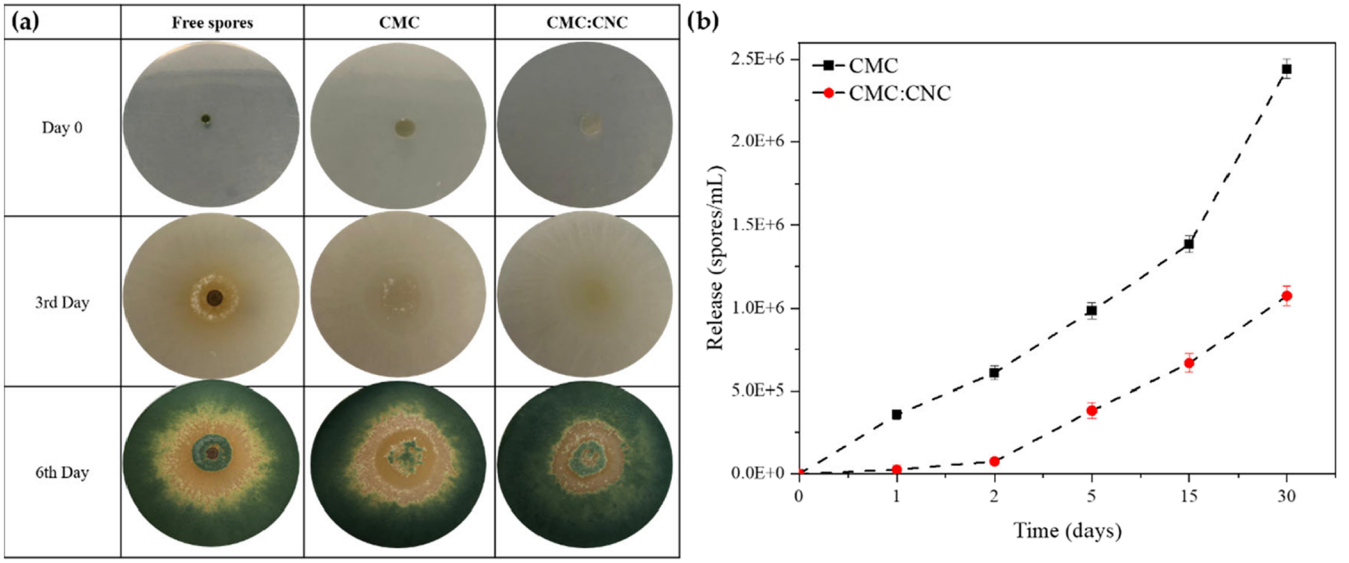

Figure 4. (a) Growth of *T. harzianum* on a Petri dish after 6 days, comparing free spores with films of CMC and CMC:CNC, illustrating the microorganism's development under different encapsulation conditions; (b) release profile of the encapsulated *T. harzianum* from CMC and CMC:CNC matrices over a 30-day period, demonstrating the release behavior of the microorganism from both matrices.

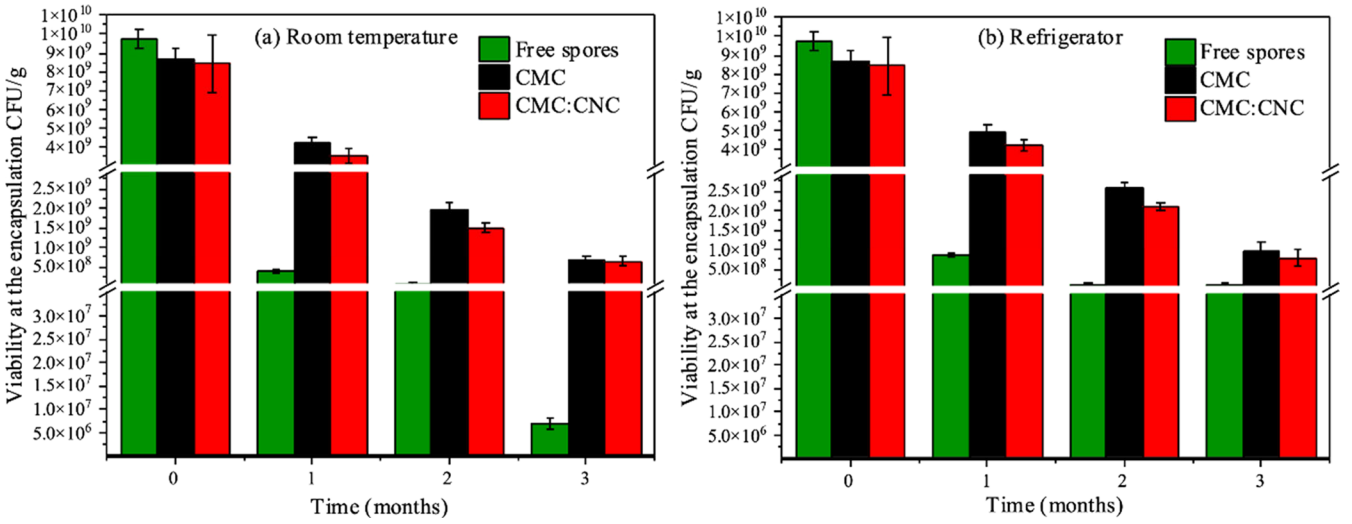

Figure 5. Viability of encapsulated *T. harzianum* in CMC and CMC:CNC matrices stored for period of 3 months. (a) Stored at room temperature; (b) stored in the refrigerator, showing the maintenance of microorganism viability under different storage conditions.

performed on films that had been stored for one month at room temperature (Figure 4a). Upon analyzing the images, similar growth rates were observed across all treatments, indicating that encapsulation did not affect fungal development. The consistent fungal growth observed suggests that the polymeric matrices effectively protected the microorganism during storage, ensuring its viability.

The release profile of *T. harzianum* in a liquid medium (saline solution of 0.85% NaCl) from CMC and CMC:CNC is presented in Figure 4b. The addition of cellulose nanocrystals (CNC) had a pronounced effect on the release rate. The CMC matrix released approximately 7.5×10^4 spores/mL after 2 h while no detectable release was observed from the CMC:CNC nanocomposite. After 15 days, the CMC matrix released 1.4×10^6 spores/mL, a value near the initial inoculated concentration (1.5×10^6 spores/mL). By day 30, the total release from the CMC matrix increased to 2.4×10^6 spores/mL, suggesting that some spores may have multiplied after release. In contrast, the CMC:CNC matrix demonstrated a significantly slower and more gradual release, reaching only 1.1×10^6 spores/mL after 30 days. This confirms that incorporating CNC into the matrix effectively delayed the diffusion of spores, creating a sustained-release system.

From an application-oriented perspective, the sustained release profile of the CMC:CNC matrix is a highly desirable feature for agricultural inoculants. Ideally, release kinetics should be tailored to the application context and the phytosanitary status of the crop. While a rapid release may be advantageous for the immediate suppression of an active disease, a sustained-release profile represents the ideal condition for preventive applications, particularly when microbial inoculants are delivered at planting.

In this preventive framework, the gradual release ensures that *T. harzianum* remains persistently present in the rhizosphere, allowing early root colonization and the establishment of a protective barrier before pathogen challenge. This

https://doi.org/10.1021/acsagscitech.5c00992
ACS Agric. Sci. Technol. 2026, 6, 527−538

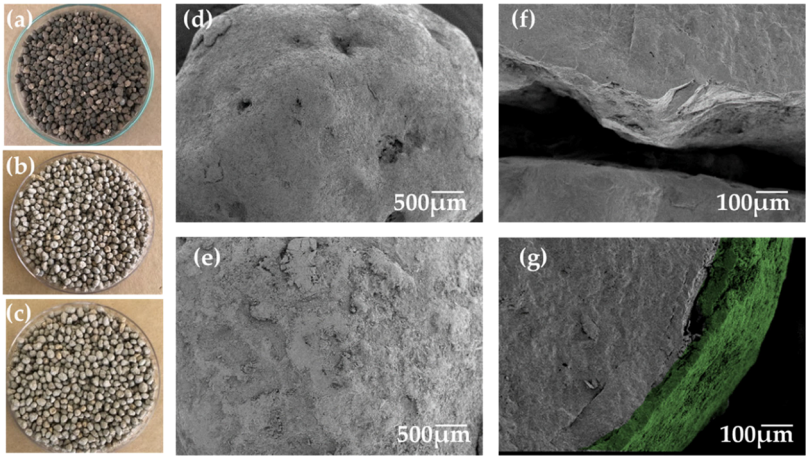

Figure 6. Appearance of granules of monoammonium phosphate (MAP) (a) uncoated; (b) coated with CMC; (c) coated with CMC:CNC. SEM image of the surface of MAP granules (d) uncoated (e) coated with CMC. SEM image of the fracture (f) coated with CMC (g) coated with CMC:CNC.

sustained presence also supports the induction of systemic resistance (priming), a well-documented mode of action of *Trichoderma spp*.[17] Furthermore, controlled delivery is essential to maintain stable microbial populations over time, avoiding the rapid population declines commonly associated with burst-release formulations.[45]

In the specific context of fertilizer coating, slow release additionally prevents the sudden exposure of spores to high osmotic stress in the vicinity of fertilizer granules, preserving microbial viability until successful establishment in the soil environment.[15,46,47] The 30-day release period observed in this study appears notably more prolonged than that of other biopolymer systems. For instance, hydrogel capsules based on alginate and pectin were shown to release the majority of their *Trichoderma* conidia within the first 5 to 72 h.[46] Similarly, chitosan-guar gum nanocomposites also demonstrated a complete release profile over a 72 h period.[45] This prolonged release behavior can be attributed to the ability of CNCs to reinforce the polymeric matrix and increase diffusion tortuosity,[47] an effect governed by strong interfacial interactions and hydrogen bonding between the CNC hydroxyl groups and the CMC chains, which anchor the active agents and prevent an initial burst release.[48] In addition, CNC incorporation reduces the free volume within the polymer network, directly affecting swelling-driven transport and further regulating the diffusion of encapsulated bio-components into the external medium.[49] Therefore, the CMC:CNC matrix is a promising candidate for developing effective inoculants that require gradual and continuous microbial delivery over time.

Viability of the Microorganism during Storage

Shelf life is a crucial factor in the commercial production of biological agents, particularly in agricultural applications, where the preservation of microorganism viability is essential for their effectiveness in the field. Encapsulation has been recognized as an effective strategy to enhance microbial stability, improving both durability and performance.

As shown in Figure 5, the encapsulation provided a significant protective effect under both storage conditions, with the most pronounced impact observed at room temperature. When stored at room temperature (≈30 °C), which represents a particularly challenging condition for microbial stability, free spores showed a severe viability loss of 3 orders of magnitude, finishing at 6.9×10^6 CFU/g. Conversely, the CMC and CMC:CNC formulations protected the microorganism, exhibiting only a one-order magnitude reduction to finish at 6.8×10^8 CFU/g and 6.4×10^8 CFU/g, respectively. Even under refrigeration (4 °C), where conditions were more favorable, the benefit of encapsulation was clear; the viability of free spores decreased by 2 orders of magnitude to 8.0×10^7 CFU/g, while the encapsulated formulations declined by only one, maintaining high counts of 9.6×10^8 CFU/g (CMC) and 7.9×10^8 CFU/g (CMC:CNC).

The enhanced stability of the encapsulated spores can be attributed to the protective properties characteristics of the polymeric matrix. The hygroscopic nature of CMC likely acted as a physical barrier, controlling water activity and mitigating osmotic stress and dehydration damage, which is a key protective mechanism for biopolymers.[50] Notably, the performance of the CMC:CNC formulations under ambient storage conditions surpassed that of conventional alginate-based systems. While our formulations exhibited only a one-order-of-magnitude reduction in viable spores after 3 months at room temperature, previous studies have reported a complete loss of viability under comparable conditions. For instance, Maruyama et al.[42] observed that *T. harzianum* encapsulated in dried alginate beads showed no detectable viability after 90 days at 30 °C, and Locatelli et al.[51] similarly reported that alginate/glycerol and alginate/polyphosphate formulations lost all viability after 2−4 months at 28 °C. In contrast, our CMC:CNC matrix maintained cell concentrations above 10^8 CFU g^{-1} after 3 months, demonstrating its protective capacity and making it an excellent candidate for inoculant formulations requiring extended shelf life under nonrefrigerated conditions.

Thus, both CMC and CMC:CNC formulations were effective in maintaining high viable cell concentrations of *T. harzianum* throughout the 3-month storage period. This is particularly relevant for microbial inoculants, as both formulations maintained viable counts within the range of 10^5 to 10^9 CFU/g, a commonly accepted standard for biological control products according to European guidelines.[52] While the new Brazilian legislation (Law No. 15.070/2024) focuses on broader regulatory frameworks rather than specific numerical thresholds, the high viability levels

https://doi.org/10.1021/acsagscitech.5c00992
ACS Agric. Sci. Technol. 2026, 6, 527−538

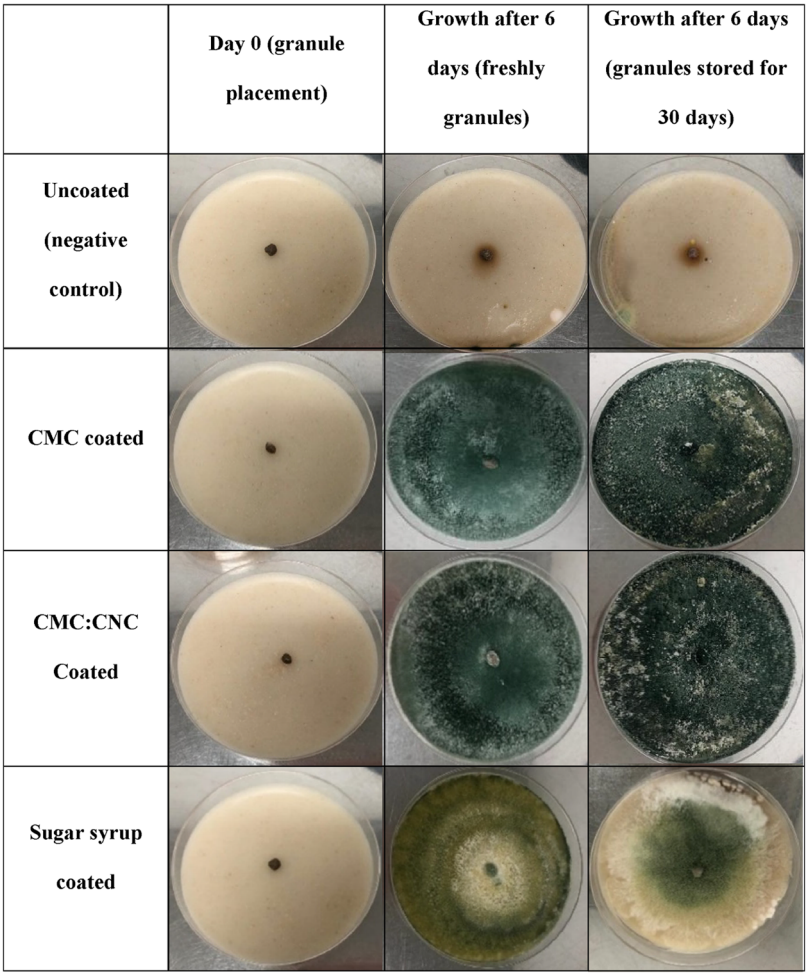

Figure 7. Growth of *T. harzianum* from MAP granules on an oatmeal agar plate. Rows represent the MAP treatments: uncoated (negative control), CMC-coated, CMC:CNC-coated, and sugar syrup−coated (farm-practice reference). Columns represent the evaluation stages: Day 0 (immediately after placement of the granule on the culture medium), fungal growth after 6 days of incubation from freshly coated granules, and fungal growth after 6 days of incubation from granules stored for 30 days at room temperature prior to testing.

maintained by these formulations are fully consistent with established international criteria for effective microbial bioinoculants.

MAP Fertilizer Coating

The successful coating of MAP fertilizer granules was confirmed by visual and microscopic analysis (Figure 6). Visually, the uncoated granules appeared brownish, while those coated with the CMC and CMC:CNC matrices exhibited a slight whitish hue. SEM revealed that the uncoated granules had a rough, porous surface (Figure 6d), whereas the coated granules were covered by a uniform polymer layer with an average thickness of approximately 20.22 μm (Figure 6g). This coating effectively smoothed the granule surface, reducing irregularities. Such improvements in surface uniformity are critical as they enhance the coating's barrier properties, which can minimize moisture penetration and reduce dust generation, typically associated with edges and nonuniformities of uncoated granules, as previously noted by Liu et al.[53]

A growth assay was performed to confirm that the coating process preserved the viability of the encapsulated fungus (Figure 7). After 6 days of incubation using freshly coated granules, the fungus exhibited robust and consistent mycelial development for both polymer-based treatments, suggesting that the polymer coatings facilitated fungal viability and colonization. As expected, no fungal growth was observed for the uncoated MAP granules (negative control), confirming that the fertilizer itself is sterile and that all fungal development observed in the other treatments originated exclusively from the intentional inoculation. These results confirm the compatibility between the biopolymeric matrices and the microorganism, reinforcing their potential use as carriers in bioformulations.

In contrast, although the sugar syrup formulation also promoted fungal proliferation when freshly prepared, the resulting colonies exhibited altered coloration and less uniform pigmentation compared with the polymer-based treatments. This behavior indicates that, while the sugar syrup allows initial fungal growth, it does not provide a structured protective environment comparable to the polymeric matrices. This variation may be attributed to differences in nutrient composition and availability provided by the sugar solution, which can influence the physiology or sporulation pattern of *T. harzianum*.

To evaluate the protective capacity of the coatings during storage, the growth assay was repeated using granules that had been stored for 30 days at room temperature (Figure 7). A significant divergence in performance was observed relative to the assay conducted using freshly coated granules. While the

https://doi.org/10.1021/acsagscitech.5c00992
ACS Agric. Sci. Technol. 2026, 6, 527−538

granules coated with the CMC and CMC:CNC matrices still supported intense and homogeneous sporulation, demonstrating effective preservation of fungal viability, the sugar syrup–coated granules exhibited sparse and irregular growth after storage, reflecting a pronounced loss of fungal viability over time due to the lack of an effective protective barrier between the microorganism and the fertilizer matrix. As expected, uncoated MAP granules again showed no fungal growth, reinforcing their role as a sterility control.

This result highlights that traditional on-farm inoculation methods, which rely on simple adhesives such as sugar solutions,[20,21] may provide limited protection against fertilizer-induced chemical stress over time. Although sugar-based stickers are widely used to facilitate initial adhesion, they do not form a robust structural barrier, leaving spores vulnerable to the high osmotic pressure generated during MAP dissolution.

To further elucidate the underlying mechanism responsible for this protective effect, the enhanced performance of polymer-coated granules can be primarily attributed to physical isolation and osmotic buffering provided by the polymeric matrix. The CMC and CMC:CNC coatings form a barrier between the microorganism and the saline and acidic microenvironment generated during fertilizer dissolution, thereby reducing exposure to osmotic shock and extreme pH conditions. This mechanism is particularly relevant for *T. harzianum*, which is sensitive to osmotic stress. In contrast, more resilient microorganisms, such as endospore-forming bacteria of the genus *Bacillus*, possess intrinsic physiological mechanisms that confer tolerance to extreme salinity and pH.[54] For these species, while encapsulation may not be essential for immediate survival, polymeric coatings can still provide functional advantages, including controlled release and protection during handling and field application.[15,55]

Taken together, this demonstrated protective capacity against fertilizer-induced stress, combined with the enhanced shelf life and sustained-release profile, confirms that the CMC:CNC nanocomposite is a robust and multifunctional platform for the encapsulation and delivery of *T. harzianum*. The developed matrices provide a protective barrier against osmotic stress, improve storage viability relative to non-encapsulated spores, and enable sustained microbial release through CNC incorporation. These combined features directly address key limitations associated with the practical deployment of microbial inoculants in fertilizer-based delivery systems.

From a practical and translational perspective, the application of the CMC:CNC coating is supported by the industrial maturity and accessibility of its components. CMC is a widely available, cost-effective biopolymer produced at industrial scale and extensively used in sustainable material applications. Regarding the cost–benefit balance of reinforcement, the use of CNCs at low concentrations (0.25% w/v) ensures that functional improvements in microbial protection and controlled release are achieved with minimal impact on the overall formulation cost.[45] Furthermore, the production of CNCs from biomass residues promotes the valorization of agro-industrial waste, aligning the proposed technology with circular bioeconomy principles.[56] Collectively, these factors indicate the potential of the proposed delivery system for the development of biofertilizers.

■ ASSOCIATED CONTENT

Supporting Information

The Supporting Information is available free of charge at https://pubs.acs.org/doi/10.1021/acsagscitech.5c00992.

Images of CMC and CMC:CNC films prepared at different concentrations for the preliminary formulation screening (PDF)

■ AUTHOR INFORMATION

Corresponding Author

Cristiane S. Farinas − *Nanotechnology National Laboratory for Agriculture, Embrapa Instrumentation, 13561-206 São Carlos, SP, Brazil; Graduate Program of Chemical Engineering, Federal University of São Carlos, 13565-905 São Carlos, SP, Brazil;* orcid.org/0000-0002-9985-190X; Email: cristiane.farinas@embrapa.br

Authors

Aline M. Ferreira − *Nanotechnology National Laboratory for Agriculture, Embrapa Instrumentation, 13561-206 São Carlos, SP, Brazil; Graduate Program of Chemical Engineering, Federal University of São Carlos, 13565-905 São Carlos, SP, Brazil*

Mariana G. Brondi − *Nanotechnology National Laboratory for Agriculture, Embrapa Instrumentation, 13561-206 São Carlos, SP, Brazil;* orcid.org/0000-0002-2228-8960

Complete contact information is available at: https://pubs.acs.org/10.1021/acsagscitech.5c00992

Funding

The Article Processing Charge for the publication of this research was funded by the Coordenacao de Aperfeicoamento de Pessoal de Nivel Superior (CAPES), Brazil (ROR identifier: 00x0ma614).

Notes

The authors declare no competing financial interest.

■ ACKNOWLEDGMENTS

The authors would like to thank the financial support provided by the São Paulo State Research Foundation (FAPESP, grants 2024/09631-8, 2025/11884-4 and 2025/03314-3), the Brazilian National Council for Scientific and Technological Development (CNPq, grants 303017/2022-8, 140341/2024-2, 402713/2023-0, 441573/2023-1, 442575/2019-0-SISNANO/MCTI program, and 406925/2022-4-INCT Circularity in Polymer Materials), the Coordination for the Improvement of Higher Education Personnel (CAPES, Finance Code 001), the Agronano Network, and the Brazilian Agricultural Research Corporation (Embrapa).

■ REFERENCES

(1) OECD|Food and Agriculture Organization of the United Nations. OECD-FAO Agricultural Outlook 2024-2033. In *OECD-FAO Agricultural Outlook*; OECD, 2024 DOI: 10.1787/4c5d2cfb-en.

(2) dos Reis, G. A.; Martínez-Burgos, W. J.; Pozzan, R.; Puche, Y. P.; Ocán-Torres, D.; de Queiroz Fonseca Mota, P.; Rodrigues, C.; Serra, J. L.; Scapini, T.; Karp, S. G.; Soccol, C. R. Comprehensive Review of Microbial Inoculants: Agricultural Applications, Technology Trends in Patents, and Regulatory Frameworks. *Sustainability* **2024**, *16* (19), No. 8720.

(3) Pathak, V. M.; Verma, V. K.; Rawat, B. S.; Kaur, B.; Babu, N.; Sharma, A.; Dewali, S.; Yadav, M.; Kumari, R.; Singh, S.; Mohapatra, A.; Pandey, V.; Rana, N.; Cunill, J. M. Current Status of Pesticide Effects on Environment, Human Health and It's Eco-Friendly Management as Bioremediation: A Comprehensive Review. *Front. Microbiol.* **2022**, *13*, No. 962619, DOI: 10.3389/fmicb.2022.962619.
(4) Serrão, C. P.; Ortega, J. C. G.; Rodrigues, P. C.; de Souza, C. R. B. Bacillus Species as Tools for Biocontrol of Plant Diseases: A Meta-Analysis of Twenty-Two Years of Research, 2000−2021. *World J. Microbiol. Biotechnol.* **2024**, *40* (4), No. 110.
(5) Rodrigues, J. S.; Takeshita, V.; Campos, E. V. R.; de Freitas, A. S. M.; de Lima, V. H.; Fraceto, L. F. Lignocellulosic Biomass in Nanopesticides: A Path toward Sustainable Agriculture. *ACS Sustainable Chem. Eng.* **2024**, *12* (27), 10045−10067.
(6) Elnahal, A. S. M.; El-Saadony, M. T.; Saad, A. M.; Desoky, E.-S. M.; El-Tahan, A. M.; Rady, M. M.; AbuQamar, S. F.; El-Tarabily, K. A. The Use of Microbial Inoculants for Biological Control, Plant Growth Promotion, and Sustainable Agriculture: A Review. *Eur. J. Plant Pathol.* **2022**, *162* (4), 759−792.
(7) Florencio, C.; Bortoletto-Santos, R.; Favaro, C. P.; Brondi, M. G.; Velloso, C. C. V.; Klaic, R.; Ribeiro, C.; Farinas, C. S.; Mattoso, L. H. C. Avanços Na Produção E Formulação De Inoculantes Microbianos Visando Uma Agricultura Mais Sustentável. *Quím. Nova* **2022**, *45*, 1133−1145.
(8) Majaron, V. F.; da Silva, M. G.; Bortoletto-Santos, R.; Klaic, R.; Ribeiro, S. J. L.; Polito, W. L.; Bevilaqua, D.; Farinas, C. S.; Ribeiro, C. Bioactive Material with Microorganisms Can Enhance the Micronutrients Solubilization and Sulfate Availability from Low Reactive Sources: Insight for Application as Coating Fertilizer Granules. *J. Polym. Environ.* **2022**, *30* (6), 2602−2613.
(9) Brondi, M.; Florencio, C.; Mattoso, L.; Ribeiro, C.; Farinas, C. Encapsulation of *Trichoderma harzianum* with Nanocellulose/Carboxymethyl Cellulose Nanocomposite. *Carbohydr. Polym.* **2022**, *295*, No. 119876.
(10) Lopes, M. M.; Lodi, L. A.; de Oliveira-Paiva, C. A.; Farinas, C. S. Emulsion/Cross-Linking Encapsulation of Bacillus in Starch/PVA-Based Microparticles for Agricultural Applications. *ACS Agric. Sci. Technol.* **2024**, *4* (4), 490−499.
(11) Løvschall, K. B.; Velasquez, S. T. R.; Kowalska, B.; Ptaszek, M.; Jarecka, A.; Szczech, M.; Wurm, F. R. Enhancing Stability and Efficacy of *Trichoderma* Bio-Control Agents Through Layer-by-Layer Encapsulation for Sustainable Plant Protection. *Adv. Sustainable Syst.* **2024**, *8* (7), No. 2300409, DOI: 10.1002/adsu.202300409.
(12) Akhlaq, M.; Mushtaq, U.; Naz, S.; Uroos, M. Carboxymethyl Cellulose-Based Materials as an Alternative Source for Sustainable Electrochemical Devices: A Review. *RSC Adv.* **2023**, *13* (9), 5723−5743.
(13) Wollerdorfer, M.; Bader, H. Influence of Natural Fibres on the Mechanical Properties of Biodegradable Polymers. *Ind. Crops Prod.* **1998**, *8* (2), 105−112.
(14) Missale, E.; Maniglio, D.; Speranza, G.; Frasconi, M.; Pantano, M. F. Cellulose Nanocrystal Composites with Enhanced Mechanical Properties for Robust Transparent Thin Films. *ACS Appl. Nano Mater.* **2024**, *7* (16), 18167−18176.
(15) Brondi, M. G.; Florencio, C.; Vasconcellos, V. M.; Ribeiro, C.; Farinas, C. S. Enhancing the Shelf Life and Stress Tolerance of the Biocontrol Agent *Trichoderma harzianum* by Encapsulation in Green Matrices of Nanocellulose and Carboxymethyl Cellulose. *ACS Agric. Sci. Technol.* **2025**, *5* (6), 1178−1188.
(16) Ding, H.; Li, X.; Wang, S.; Yang, Y.; Chen, X.; Chen, C.; Wang, H.*Trichoderma harzianum* for the Control of Agricultural Pests: Potential, Progress, Applications and Future Prospects *Rev. Argent. Microbiol.* 2025 .
(17) Chen, X.; Lu, Y.; Liu, X.; Gu, Y.; Li, F. *Trichoderma*: Dual Roles in Biocontrol and Plant Growth Promotion. *Microorganisms* **2025**, *13* (8), No. 1840.
(18) Geng, Y.; Chen, S.; Lv, P.; Li, Y.; Li, J.; Jiang, F.; Wu, Z.; Shen, Q.; Zhou, R. Positive Role of *Trichoderma harzianum* in Increasing Plant Tolerance to Abiotic Stresses: A Review. *Antioxidants* **2025**, *14* (7), No. 807.
(19) Contreras-Soto, M. B.; Tovar-Pedraza, J. M.; Solano-Báez, A. R.; Bayardo-Rosales, H.; Márquez-Licona, G. Biocontrol Strategies Against Plant-Parasitic Nematodes Using *Trichoderma Spp.*: Mechanisms, Applications, and Management Perspectives. *J. Fungi* **2025**, *11* (7), No. 517.
(20) O'Callaghan, M.; Ballard, R. A.; Wright, D. Soil Microbial Inoculants for Sustainable Agriculture: Limitations and Opportunities. *Soil Use Manage.* **2022**, *38* (3), 1340−1369.
(21) Sales, L. R.; Silva, A. O.; Sales, F. R.; Rodrigues, T. L.; Barbosa, M. V.; Santos, J. V. D.; Kemmelmeier, K.; Siqueira, J. O.; Carneiro, M. A. C. On Farm Inoculation of Native Arbuscular Mycorrhizal Fungi Improves Efficiency in Increasing Sugarcane Productivity in the Field. *Rhizosphere* **2022**, *22*, No. 100539.
(22) Rojas-Sánchez, B.; Guzmán-Guzmán, P.; Morales-Cedeño, L. R.; del Carmen Orozco-Mosqueda, M.; Saucedo-Martínez, B. C.; Sánchez-Yáñez, J. M.; Fadiji, A. E.; Babalola, O. O.; Glick, B. R.; Santoyo, G. Bioencapsulation of Microbial Inoculants: Mechanisms, Formulation Types and Application Techniques. *Appl. Biosci.* **2022**, *1* (2), 198−220.
(23) Bortoletto-Santos, R.; Ribeiro, C.; Polito, W. L. Controlled Release of Nitrogen-Source Fertilizers by Natural-Oil-Based Poly(Urethane) Coatings: The Kinetic Aspects of Urea Release. *J. Appl. Polym. Sci.* **2016**, *133* (33), No. 43790, DOI: 10.1002/app.43790.
(24) Peng, Y.; Via, B. The Effect of Cellulose Nanocrystal Suspension Treatment on Suspension Viscosity and Casted Film Property. *Polymers* **2021**, *13* (13), No. 2168.
(25) Muñoz-Celaya, A. L.; Ortiz-García, M.; Vernon-Carter, E. J.; Jauregui-Rincón, J.; Galindo, E.; Serrano-Carreón, L. Spray-Drying Microencapsulation of *Trichoderma harzianum* Conidias in Carbohydrate Polymers Matrices. *Carbohydr. Polym.* **2012**, *88* (4), 1141−1148.
(26) Oun, A. A.; Rhim, J.-W. Characterization of Carboxymethyl Cellulose-Based Nanocomposite Films Reinforced with Oxidized Nanocellulose Isolated Using Ammonium Persulfate Method. *Carbohydr. Polym.* **2017**, *174*, 484−492.
(27) El-Sayed, S.; Mahmoud, K. H.; Fatah, A. A.; Hassen, A. DSC, TGA and Dielectric Properties of Carboxymethyl Cellulose/Polyvinyl Alcohol Blends. *Phys. B* **2011**, *406* (21), 4068−4076.
(28) Mallakpour, S.; Abdolmaleki, A.; Khalesi, Z.; Borandeh, S. Surface Functionalization of GO, Preparation and Characterization of PVA/TRIS-GO Nanocomposites. *Polymer* **2015**, *81*, 140−150.
(29) D'Acierno, F.; Michal, C. A.; MacLachlan, M. J. Thermal Stability of Cellulose Nanomaterials. *Chem. Rev.* **2023**, *123* (11), 7295−7325.
(30) Kumar, B.; Kumar, S.; Kim, J. Novel Carboxymethyl Cellulose-Grafted Polyacrylic Acid/Cellulose Nanocrystal Nanocomposite Materials as Bio-Based Adhesive. *Mater. Today Commun.* **2024**, *38*, No. 108497.
(31) Yadav, M.; Behera, K.; Chang, Y.-H.; Chiu, F.-C. Cellulose Nanocrystal Reinforced Chitosan Based UV Barrier Composite Films for Sustainable Packaging. *Polymers* **2020**, *12* (1), No. 202, DOI: 10.3390/polym12010202.
(32) Mandal, A.; Chakrabarty, D. Studies on Mechanical, Thermal, and Barrier Properties of Carboxymethyl Cellulose Film Highly Filled with Nanocellulose. *J. Thermoplast. Compos. Mater.* **2019**, *32* (7), 995−1014.
(33) Li, H.; Shi, H.; He, Y.; Fei, X.; Peng, L. Preparation and Characterization of Carboxymethyl Cellulose-Based Composite Films Reinforced by Cellulose Nanocrystals Derived from Pea Hull Waste for Food Packaging Applications. *Int. J. Biol. Macromol.* **2020**, *164*, 4104−4112.
(34) Zoppe, J. O.; Johansson, L.-S.; Seppälä, J. Manipulation of Cellulose Nanocrystal Surface Sulfate Groups toward Biomimetic Nanostructures in Aqueous Media. *Carbohydr. Polym.* **2015**, *126*, 23−31.
(35) El Achaby, M.; El Miri, N.; Hannache, H.; Gmouh, S.; Ben youcef, H.; Aboulkas, A. Production of Cellulose Nanocrystals from

Vine Shoots and Their Use for the Development of Nanocomposite Materials. *Int. J. Biol. Macromol.* **2018**, *117*, 592−600.
(36) Shetty, S. K.; Ismayil; Nasreen; Swathi; Mahesha, M. G.; Keshav, R. Sodium Ion Conducting PVA/NaCMC Bio Poly-Blend Electrolyte Films for Energy Storage Device Applications. *Int. J. Polym. Anal. Charact.* **2021**, *26* (5), 411−424.
(37) Zheng, W. J.; Gao, J.; Wei, Z.; Zhou, J.; Chen, Y. M. Facile Fabrication of Self-Healing Carboxymethyl Cellulose Hydrogels. *Eur. Polym. J.* **2015**, *72*, 514−522.
(38) Yadollahi, M.; Namazi, H.; Barkhordari, S. Preparation and Properties of Carboxymethyl Cellulose/Layered Double Hydroxide Bionanocomposite Films. *Carbohydr. Polym.* **2014**, *108*, 83−90.
(39) Jasmani, L.; Adnan, S. Preparation and Characterization of Nanocrystalline Cellulose from *Acacia mangium* and Its Reinforcement Potential. *Carbohydr. Polym.* **2017**, *161*, 166−171.
(40) Kusmono; Listyanda, R. F.; Wildan, M. W.; Ilman, M. N. Preparation and Characterization of Cellulose Nanocrystal Extracted from Ramie Fibers by Sulfuric Acid Hydrolysis. *Heliyon* **2020**, *6* (11), No. e05486, DOI: 10.1016/j.heliyon.2020.e05486.
(41) Bet, M. R.; Goissis, G.; Lacerda, C. A. Characterization of Polyanionic Collagen Prepared by Selective Hydrolysis of Asparagine and Glutamine Carboxyamide Side Chains. *Biomacromolecules* **2001**, *2* (4), 1074−1079.
(42) Maruyama, C. R.; Bilesky-José, N.; de Lima, R.; Fraceto, L. F. Encapsulation of Trichoderma harzianum Preserves Enzymatic Activity and Enhances the Potential for Biological Control. *Front. Bioeng. Biotechnol.* **2020**, *8*, No. 225, DOI: 10.3389/fbioe.2020.00225.
(43) Eichers, M.; Bajwa, D.; Shojaeiarani, J.; Bajwa, S. Biobased Plasticizer and Cellulose Nanocrystals Improve Mechanical Properties of Polylactic Acid Composites. *Ind. Crops Prod.* **2022**, *183*, No. 114981.
(44) Gong, J.; Li, J.; Xu, J.; Xiang, Z.; Mo, L. Research on Cellulose Nanocrystals Produced from Cellulose Sources with Various Polymorphs. *RSC Adv.* **2017**, *7*, 33486−33493, DOI: 10.1039/C7RA06222B.
(45) Sangeetha, B. M.; Chandrika, K. S. V. P.; Prasad, R. D.; Bhat, B. N.; V, D. K. Copper Doped Chitosan-Guar Gum Nanocomposite: A Multifunctional Carrier for *Trichoderma* with Potent Antifungal Properties. *Int. J. Biol. Macromol.* **2025**, *311*, No. 143919.
(46) Cruz-Barrera, M.; Izquierdo-García, L. F.; Gómez-Marroquín, M.; Santos-Díaz, A.; Uribe-Gutiérrez, L.; Moreno-Velandia, C. A. Hydrogel Capsules as New Delivery System for *Trichoderma koningiopsis* Th003 to Control Rhizoctonia Solani in Rice (Oryza Sativa). *World J. Microbiol. Biotechnol.* **2024**, *40* (4), 108.
(47) Dogaru, B.-I.; Stoleru, V.; Mihalache, G.; Yonsel, S.; Popescu, M.-C. Gelatin Reinforced with CNCs as Nanocomposite Matrix for *Trichoderma harzianum* KUEN 1585 Spores in Seed Coatings. *Molecules* **2021**, *26* (19), No. 5755.
(48) de S M de Freitas, A.; Rodrigues, J. D. S.; Municoy, S.; Antezana, P. E.; Desimone, M. F.; Foresti, M. L.; Ferreira, M.; Lemes, A. P. Nanostructured TPS/PVA/CNC Films for Sustained Copper Oxide Nanoparticle Release: Toward Advanced Transdermal Dressing Systems. *Int. J. Pharm.* **2025**, *675*, No. 125558.
(49) Kasbi, K.; Nazemi, Z.; Janmohammadi, M.; Bahraminasab, M.; Arabhalvaei, M.; Nourbakhsh, M. S. Tuning Antibiotic Release from Gelatin-Cellulose Nanocrystal Hydrogel Films. *Int. J. Biol. Macromol.* **2025**, *329*, No. 147743.
(50) Oun, A. A.; Rhim, J.-W. Characterization of Carboxymethyl Cellulose-Based nanocomposite Films Reinforced with Oxidized Nanocellulose Isolated Using Ammonium Persulfate Method. *Carbohydr. Polym.* **2017**, *174*, 484−492.
(51) Locatelli, G. O.; dos Santos, G. F.; Botelho, P. S.; Finkler, C. L. L.; Bueno, L. A. Desenvolvimento de Formulações de Trichoderma Sp. Em Grânulos Encapsulados (CG) e Avaliação Da Vida Útil Dos Conídios. *Biol. Control* **2018**, *117*, 21−29.
(52) Natsiopoulos, D.; Tziolias, A.; Lagogiannis, I.; Mantzoukas, S.; Eliopoulos, P. A. Growth-Promoting and Protective Effect of *Trichoderma* Atrobrunneum and T. Simmonsii on Tomato against Soil-Borne Fungal Pathogens. *Crops* **2022**, *2* (3), 202−217.
(53) Liu, Q.; Meng, X.; Li, T.; Raza, W.; Liu, D.; Shen, Q. The Growth Promotion of Peppers (Capsicum Annuum L.) by *Trichoderma* Guizhouense NJAU4742-Based Biological Organic Fertilizer: Possible Role of Increasing Nutrient Availabilities. *Microorganisms* **2020**, *8* (9), No. 1296.
(54) Mantea, L.-E.; El-Sabeh, A.; Mihasan, M.; Stefan, M. Bacillus Safensis P1.5S Exhibits Phosphorus-Solubilizing Activity Under Abiotic Stress. *Horticulturae* **2025**, *11* (4), No. 388.
(55) Arias-Chavarría, L. D.; Batista-Menezes, D.; Orozco-Cayasso, S.; Vargas-Martínez, A.; Vega-Baudrit, J. R.; de Oca-Vásquez, G. M. Evaluation of the Viability of Microencapsulated *Trichoderma* Longibrachiatum Conidia as a Strategy to Prolong the Shelf Life of the Fungus as a Biological Control Agent. *Front. Chem.* **2025**, *12*, No. 1473217, DOI: 10.3389/fchem.2024.1473217.
(56) Esquivel-Alfaro, M.; Rojas-Carrillo, O.; Sulbarán-Rangel, B.; Rodríguez-Barquero, L.; Palacios-Hinestroza, H.; Rojas, O. J. Pineapple-Derived Nanocellulose for Nanocomposites: Extraction, Processing, and Properties. *J. Compos. Sci.* **2025**, *9* (12), No. 652.